VALIDATION OF THE CONTROL STRATEGY OF THE FREE FLYING ROBOT – APPLICATION TO THE RENDEZVOUS MANOEUVRES

Karol Seweryn[1], Tomasz Barciński[1,2], Monika Ciesielska[1], Jerzy Grygorczuk[1], Tomasz Rybus[1], Konrad Skup[1], Roman Wawrzaszek[1]

[(1)] *Space Research Centre of the Polish Academy of Sciences, Bartycka 18a str., 00-716 Warsaw, Poland, kseweryn@cbk.waw.pl*

[(2)] *West Pomeranian University of Technology, Piastów 17 av., 70-310 Szczecin, Poland*

ABSTRACT

Orbital maneuvers like rendezvous and docking to the target satellite and so called close proximity spacecraft-asteroid maneuvers require careful planning and subsequent control of motion of a space robot (spacecraft equipped with manipulator arm). Such maneuvers constitute an important part of the future orbital servicing systems dedicated to (i) geostationary and low Earth orbit as well as (ii) missions to the small asteroids. In both cases the main goal of the space robot operation is to localize its end effector in some specified point in target body frame.

In this paper it was analyzed two navigation scenarios; in the first case the end effector has to be positioned in predefined point in target frame at the final time. In the second case the end effector has to realized predefined trajectory in the target frame in specified time frame. In both case the maneuvers are characterized by its relatively short time (tens of seconds) and control system based on joint angle measurements. The analysis was based on numerical simulation and compared with test results obtained on air bearing test-bed system.

1. INTRODUCTION

The lifetime of satellites is sometimes significantly shortened by various malfunctions (e.g., failures of attitude control systems, failures of deployment mechanisms [1]). Spacecraft equipped with a manipulator arm could be used for performing on-orbit servicing missions and prolonging operational period of commercial satellites (e.g., [2], [3], [4]). Very challenging stage of servicing missions is the capture manoeuvres, in which the robotic arm must be used for capturing target satellite (especially in case of uncontrolled target). During this manoeuvre interaction occurring between the servicing satellite and the robotic arm must be taken into account by the control system [5]. A servicing satellite capable of capturing non-cooperative uncontrolled targets may also be used for capturing and removing from orbit large space debris (i.e., defunct, defective satellites). Concepts of such missions are proposed (e.g., [6]). The number of simulations results were presented also by authors of this paper on previous conferences [7], [8].

The sample return missions are one option to extend our knowledge about the extra-terrestrial materials, processes occurring on surface and subsurface level, as well as interactions between such materials and mechanisms developed technology. This knowledge is supporting scientific investigations connected with NEA (Near-Earth Asteroids) and discussion about origin of the Solar System. In the past there were several robotic mission intended to deliver to Earth extra-terrestrial materials, e.g., Hayabusa mission to Itokawa and unsuccessful Phobos Grunt mission together with CHOMIK sampling mechanism onboard [9]. Several new missions are currently planned: ESA Phootprint mission to the Phobos, ESA MarcoPolo-R mission to the NEA 1996 FG3 [10], Hayabusa 2 mission to NEA 1999 and OSIRIS-Rex to the primitive NEA 1999 RQ36. Some of this mission utilize so called “touch and go” approach to take a sample from the asteroid surface. This maneuver can be executed using robotic arm and in that sense is similar to the servicing maneuvers.

Both problems was analysed numerically using previously developed simulation tool [11], [12]. The servicing satellite is modeled as a rigid body. The specific use of SimMechanics built-in block of 6DOF joint allows simulation of rotational and translational motion of this chase spacecraft and target satellite. The robotic arm mounted on the chaser spacecraft is modeled as a chain of rigid bodies connected by rotational joints.

It is difficult to perform tests of the free-floating satellite-manipulator system on Earth, as in Earth gravitational conditions it is difficult to simulate the influence of manipulator motions on the satellite position and orientation. However, various solutions exists that allow such tests with certain limitations [13]. One possible approach is based on the planar air-bearing table. In such approach two-dimensional motion of a satellite mock-up with planar manipulator is possible, thus microgravity conditions and free-floating nature of the system can be simulated in two dimensions. New planar air-bearing microgravity simulator was constructed recently in the Space Research Centre of the Polish Academy of Sciences [14]. This new test-bed has

large area for the experiment and allows tests of heavy manipulators, as separate air-bearings are used for supporting each link of the robotic arm.

In this paper the navigation of the space robot with application to the servicing systems and spacecraft-asteroid systems is discussed. Following introduction, the basic theory of the free flying manipulators are presented. In the next section three different type of space robots and effector trajectories are introduced followed by short description of the air bearing test-bed system. In the section 4 the results from simulations and tests are shown. Finally the conclusion and future improvements of the system are given.

2. SPACE ROBOTS MANOUVERS DEFINITION

There is a variety of approaches for controlling the space robots [15]. They depend on the task of the manipulator arm as well as on the measurement equipment on board. The tasks can be distinguish for tasks defined in the inertial or other (e.g., target) body frame or tasks defined in the chaser body frame or in the joint space. Usually the tasks defined in the inertial space require the measurement system giving information in such frame but from technological point of view it is often a challenging tasks. Therefore, in this paper we focused on the analysis of the motion of the space robots executing the path predefined in the inertial space but with measurement system giving information only in the chaser body frame, e.g., encoders in the joints.

In the considered scenario, generalized equations of motion (1) for a mechanical system consisting of a free-flying satellite on the Earth's orbit equipped with 6 DOF robotic arm were derived from the second kind Lagrangian equations in quasi coordinates:

$$M(q)\ddot{q} + C(\dot{q},q)\dot{q} + g(q) = \tau \tag{1}$$

where $q = [r_s, e_s, \theta_1, ..., \theta_6]^T$ is a state vector consisting in the position and orientation of the satellite and manipulator joint angles. It's derivatives $\dot{q} = [v_s, \omega_s, \dot{\theta}_1, ..., \dot{\theta}_6]^T$ consisting in linear and angular velocity of the satellite in its body frame and joint angular velocities. M is a mass matrix, C is a Coriolis matrix, g is a gravity force vector and τ is a vector of generalized torques acting on the system. The torque in the joints needed to move the system from its initial state $q(t_i)$ to the final one $q(t_f)$ was computed in two different ways, however for both case first the relation between desired end effector trajectory $[r_{ee}, e_{ee}]$ and joint angle $\theta(t)$ has to be clarified.

The space robots is typically considered as a underactuated system (nonholonomic system) therefore the derivation of the torques τ requires additional assessment. Assuming that we know the desired end effector trajectory $\{r_{ee}, e_{ee}\}$, all geometrical and mass properties of a spacecraft and attached manipulator the kinematic relation between:

- linear and angular velocity of the manipulator's end effector $\{v_{ee}, \omega_{ee}\}$,
- the satellite velocities $\{v_s, \omega_s\}$ and
- manipulator joint velocities $\{\dot{\theta}\}$

in vector notation reads:

$$\begin{Bmatrix} v_{ee} \\ \omega_{ee} \end{Bmatrix} = [J_s]\begin{Bmatrix} v_s \\ \omega_s \end{Bmatrix} + [J_M]\{\dot{\theta}\} \tag{2}$$

where J_s and J_m are the Jacobions of the spacecraft and of the manipulator respectively. The kinetic energy T of the spacecraft-manipulator system takes the form:

$$T = \frac{1}{2}\begin{Bmatrix} v_s \\ \omega_s \\ \dot{\theta} \end{Bmatrix}^T \underbrace{\begin{bmatrix} [A] & [B] & [C] \\ [B]^T & [E] & [F] \\ [C]^T & [F]^T & [N] \end{bmatrix}}_{M} \begin{Bmatrix} v_s \\ \omega_s \\ \dot{\theta} \end{Bmatrix}, \tag{3}$$

where the submatrices $A,...,N$ were defined originally in [16]. The momentum P and the angular momentum L vectors of the satellite-manipulator system are:

$$\begin{Bmatrix} \{P\} \\ \{L_0\} + \{r_s\} \times \{P\} \end{Bmatrix} = \underbrace{\begin{bmatrix} [A] & [B] \\ [B]^T + [\tilde{r}_s][A] & [E] + [\tilde{r}_s][B] \end{bmatrix}}_{H_2} \begin{Bmatrix} v_s \\ \omega_s \end{Bmatrix} +$$

$$\underbrace{\begin{Bmatrix} [C] \\ [F] + [\tilde{r}_s][C] \end{Bmatrix}}_{H_3} \{\dot{\theta}\} = \begin{Bmatrix} f_p \\ f_{mp} \end{Bmatrix}, \tag{4}$$

where the angular momentum $L = L_0 + r_s x P$. In this approach the momentum and angular momentum are not conserved nor equal to zero, but are described by the time dependent functions f_p and f_{mp} that correspond to the amount of momentum and angular momentum delivered to or taken from the system:

$$\begin{Bmatrix} f_p \\ f_{mp} \end{Bmatrix} = \begin{Bmatrix} f_p(t_0) + \int \{F_s\}\, dt \\ f_{mp}(t_0) + \int \{H_s\} + [\tilde{r}_s]\{F\}_s\, dt \end{Bmatrix}, \tag{5}$$

Here F_s and H_s are the predefined force and the torque that are exerted on the servicing satellite by its thrusters. The details of these derivation can be found in [12].

Equation (4) can be considered as Pfaff-type constraints that explicitly depend on time, therefore describe the Pfaff form with drift. After decomposition and transformations the sought relation between the angular velocities of the joint and the end-effector velocity can be obtained:

$$\{\dot{\theta}\} = \left([J_M] - [J_S][H_2]^{-1}[H_3]\right)^{-1}\left(\begin{Bmatrix} v_{ee} \\ \omega_{ee} \end{Bmatrix} - [J_S][H_2]^{-1}\begin{Bmatrix} f_p \\ f_{mp} \end{Bmatrix}\right) \tag{6}$$

and after numerical integration it is possible to obtain $\theta(t)$ and satellite position and orientation $[r_s, e_s]$.

Once the joint angle $\theta(t)$ time history and its derivatives is known the generalized torque $\tau=[F_s, H_s, \tau_{ee}]$ is can be obtained either by solving invert dynamics problem (Eq. 1) or defining the controller which try to keep desired $\theta(t)$ and $d\theta(t)/dt$ during motion. The first case is an ideal one and it is treated as a reference solution. In the second case the torque τ is defined as:

$$\begin{bmatrix} F_s \\ H_s \\ \tau_{ee} \end{bmatrix} = \begin{bmatrix} 0_{6x6} & 0_{6x12} \\ 0_{3x6} & K_{3x12} \end{bmatrix} \begin{Bmatrix} 0_{6x1} \\ \theta_{ref} - \theta \\ \dot{\theta}_{ref} - \dot{\theta} \end{Bmatrix} \quad (7)$$

The control system represented by K matrix in Eq. 6 is trying to keep the joint positions and velocities as close as possible to the reference one. Due to the errors and inaccuracies an error between the reference end-effector path is continuously growing. The control system is based on the linear state-feedback, but due to system underactuation the feedback is only partial, and it operates in the configuration angles space. From another point of view the control law can be interpreted as a classical linear PD controller, which has a good performance when it is working with inertial-type plants. In the case of space robots, in presence of microgravity, the manipulator dynamics is locally approximated by the second order time integration. Therefore a good control performance can be achieved by using matrix K gains of high values, which corresponds to high frequency and damping, short raising and settling time of the control system.

The theoretical approach presented in this section was used in two different examples presented in next subsections. First one is connected with servicing manoeuvre and the second with spacecraft asteroid manoeuvre. The both application is totally different however from the theory point of view the only difference is that first one can be solved assuming zero initial momentum of the system (Eq. 4) when the second application require full solution.

2.1. On-orbit servicing manoeuvres

In this analysis the final phase of the orbital rendezvous maneuver, when servicing satellite is in close proximity to the target satellite was considered. In most general scenario four main stages of this phase can be distinguished: (i) unfolding and initial positioning of the manipulator, (ii) capturing rotating target satellite, (iii) deceleration of manipulator joints (resulting in deceleration of the target satellite angular velocity – so called 'detumbling') and (iv) positioning captured satellite. The particular attention was focused on phase (ii) which was divided into two substages:

- in the first one the manipulator arm starts from arbitrary initial position (point A in the Fig. 1) at the time t_A and move to the predefined point B in target reference frame at the time t_B. The end effector trajectory between these points are not relevant.
- in the second stage the manipulator arm continue from point B toward point C on predefined trajectory (in this case straight line) in target reference frame

The simulation view of the two first stages of such maneuvers is presented in the Fig. 1.

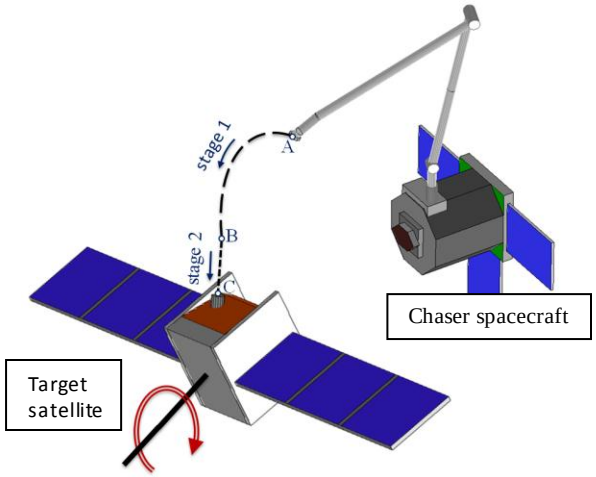

Figure 1. Two stages of the RVD maneuver: stage 1 - unfolding to the initial position and stage 2 - capturing tumbling satellite

2.2. Spacecraft-asteroid rendezvous manoeuvres

In this maneuver's type the manipulator arm is working in close proximity (single meters) of the asteroid surface when spacecraft body is moving on its orbit with relative speed in range of cm/s. The manipulator arm cooperates with sampling mechanism which allow to take the sample within 10-30 seconds.

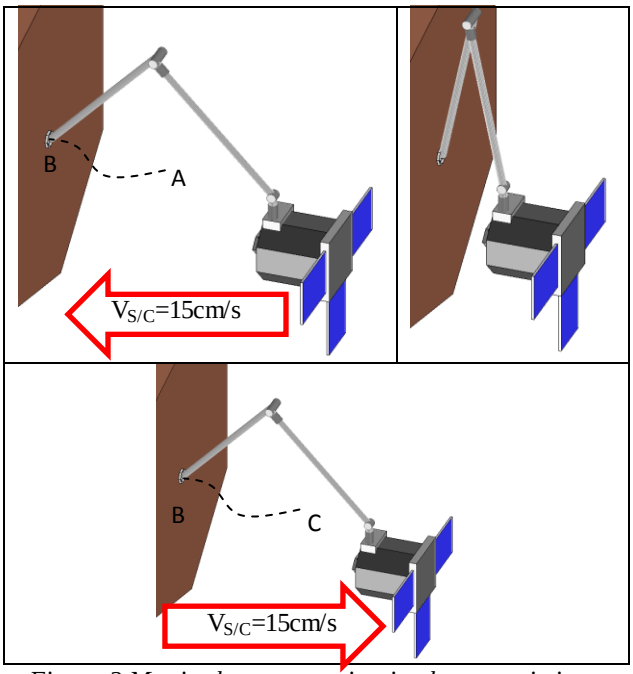

Figure 2 Manipulator operation in close proximity to the asteroid surface

The maneuver can be divided into three phases:

- Assuming that at the initial moment the spacecraft has linear velocity toward the asteroid, the end effector moves from initial point A to predefined point B in asteroid frame
- Manipulator end effector keep the constant point B during certain time. That time interval can be used for surface sampling and simultaneously, at the same time to change to spacecraft velocity into opposite direction
- Manipulator moves from point B to point C

The artistic view of this kind of manoeuvre is presented on figure 2

3. VALIDATION TOOLS

3.1 Motion manoeuvres simulator

All manoeuvres described in section 3 were analysed numerically using previously developed simulation tool [11] and [12]. The overview of Simulink model of the servicing satellite is presented in the Fig. 3. The servicing satellite is modeled as a rigid body. The specific use of SimMechanics built-in block of 6DOF joint allows simulation of rotational and translational motion of this satellite (e.g., orbital motion around the Earth under the force of gravity). The target satellite is also modeled as a rigid body connected to the ground by 6DOF joint which allows to set e.g. tumbling motion. The robotic arm mounted on the chaser spacecraft is modeled as a chain of rigid bodies connected by rotational joints.

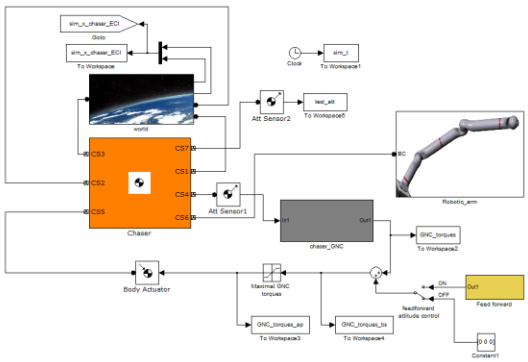

Figure 3. Overview of Simulink model of the chaser spacecraft

3.2 Air bearing test-bed system

New planar air-bearing microgravity simulator recently constructed in the Space Research Centre PAS [14] consists of flat and precisely levelled granite table. On the table satellite mock-up with 2DoF planar manipulator is placed. Satellite-manipulator system is mounted on planar air-bearings, which generate a thin film of pressurized air and slide on it. These air-bearings, supplied from the gas canister attached to the satellite mock-up, allow almost frictionless two-dimensional motion of the system. Satellite mock-up is supported on three air-bearings, while additional air-bearings are used to support independently each manipulator link, thus allowing tests of system with long and heavy manipulator. Mass of the satellite mock-up is 12.9 kg, while mass of the manipulator is 6 kg (mass of the entire system is 18.9 kg). Total length of the manipulator is 1.22 m. Picture of this system is presented in the Fig. 3 .Large area of the granite table (2x3 meters) allows tests of complex maneuvers and gives possibility of future application of flexible manipulator links.

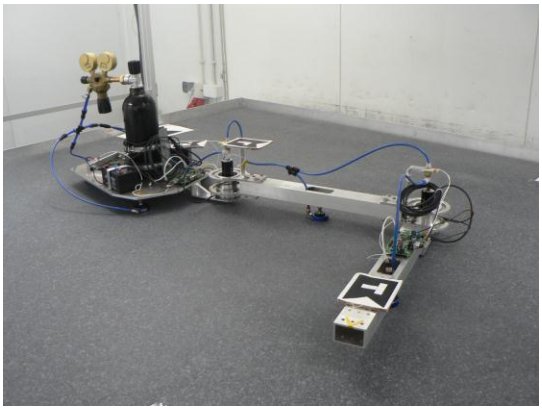

Figure 4 Planar air-bearing microgravity simulator.

Manipulator links and satellite mock-up are made from aluminum. Both manipulator joints are rotational. Each joint consists of a DC motor, harmonic drive, two resilient suspension plates and absolute optical encoder. Suspension plates are used for compensation of possible vertical misalignments between components of the system (all five air-bearings supporting the system must be ideally coplanar). The electronic subsystem consist of two kinds of electronic circuits: On Board Computer (OBC) and two joint-controller boards (JC). The OBC performs mode management and trajectory planning. It also monitors, collects and stores all the data that comes from the executive subsystems. Joint-controllers are responsible for control of the motor and for monitoring the joints position through reading the encoders. The main electronic board containing On Board Computer (OBC), joint-controller board (JC) for the first joint and batteries are attached to the satellite mock-up, while joint-controller board for the second joint is attached to the first manipulator link. Wireless Bluetooth communication is used to transmit data and commends to OBC, as any wires connecting the moving base with the external computer would affect free motion of the satellite-manipulator system. Visual pose estimation system is used to track the satellite-manipulator system during the experiment. This system provides position and orientation of both manipulator links and of manipulator base.

4. RESULTS OF THE VALIDATION

The results of validation are presented for 3 different cases. The first one includes the analysis of the closed path trajectory in joint space. The results from the simulator and the test-bed system are provided. In that his case, the trajectory is equivalent to the servicing maneuver – stage 1. The second case provides the analysis of the system motion during servicing maneuver. The analysis were done also on both levels but here only results from one simulation are presented (The test results are given in Tomasz Rybus et al. [14].) The third case presents an overview of the "touch and go" maneuvers in close proximity of the asteroid.

4.1 CASE A Close Path Trajectory

For verification of the planar air-bearing experiment modified planar version of the Simulation Tool was used. Simulations were performed with mass and geometrical properties of the satellite-manipulator system used on the test-bed. Trajectory was defined in the configuration space. Reference positions of manipulator joints used in the simulation are presented in the Fig. 5 - only the first joint was performing motion. Resulting end-effector trajectory in the Cartesian space is presented in the Fig. 6 (wrt. time) and Fig. 7 (x-y plot), while end-effector orientation is presented in the Fig. 8 The experimental results give a preliminary confirmation of the consistency between the test-bed and simulated mathematical model.

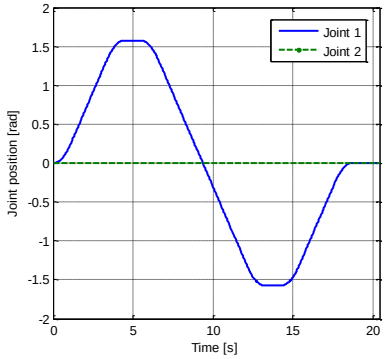

Figure 5 Reference positions of manipulator joints used in the simulation.

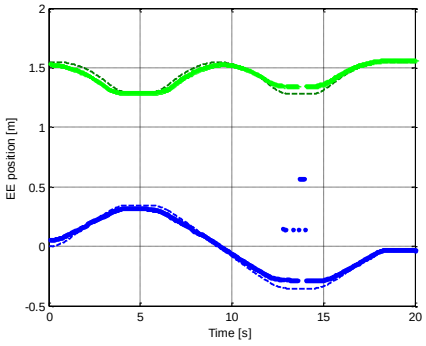

Figure 6 End-effector position in Cartesian space (x – blue, y – green), dashed line – simulations, solid line – experiments results

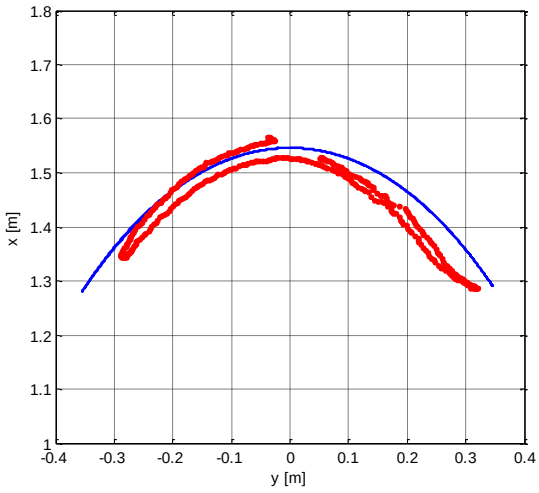

Figure 7 End-effector position in Cartesian space (blue – simulations results, red – experimental results)

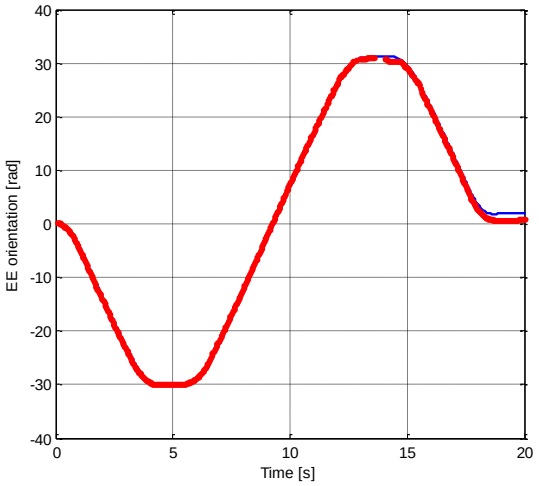

Figure 8 End-effector orientation (blue – simulations results, red – experimental results)

4.2 CASE B - Satellite servicing – capturing tumbling target

In the second case capturing target satellite by the manipulator-equipped servicing spacecraft was analysed. Geometrical and mass properties of the spacecraft-manipulator system are presented in the Tab. 1. Target satellite is in the rotational motion (tumbling) and has linear velocity in respect to the servicing satellite (0.051 m/s).

Table 1 Geometrical and mass properties of the spacecraft-manipulator system

Parameter	Value
Spacecraft mass	100 kg
Spacecraft inertia [IXX, IYY, IZZ]	[2.83; 6.08; 7.42] kg·m2
Mass of the manipulator	20 kg
Total length of the manipulator	1.92 m
Number of manipulator joints	6

Euler angles describing orientation of the target satellite are presented in the Fig. 9 . In the proposed approach end-effector trajectory during the final capture is divided into two stages: (i) initial motion of the end-effector to a position that is relatively close to the target satellite docking port (point B in Fig. 1) and (ii) linear motion (in the docking port CS) from that position to the docking port (point C in Fig. 1). Servicing satellite is in free-floating mode during the capture, therefore its position and orientation is not controlled – this fact is taken into account during trajectory planning. End-effector trajectory in the inertial reference frame located at the initial position of the servicing satellite centre of mass is presented in the Fig. 10 . Relative distance and relative velocity between the end-effector and target satellite docking port are presented in the Fig. 11, where two stages of the approach can be easily distinguished, as from 12th to 17th second end-effector is approaching docking port with constant relative velocity. Positions of first three manipulator joints are shown in the Fig. 12, while orientation of the servicing satellite is presented in the Fig. 13. Changes in the servicing satellite orientation are induced only by the motion of the manipulator during the manoeuvre.

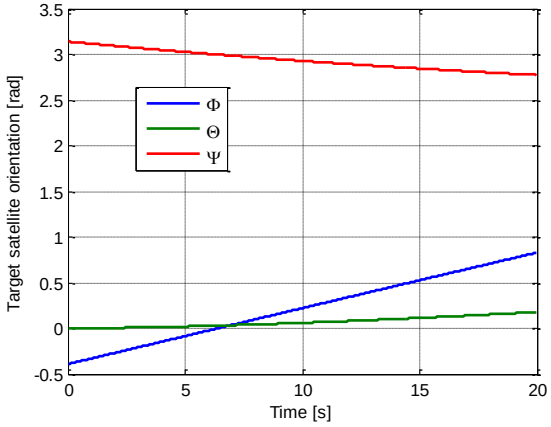

Figure 9 Target satellite orientation

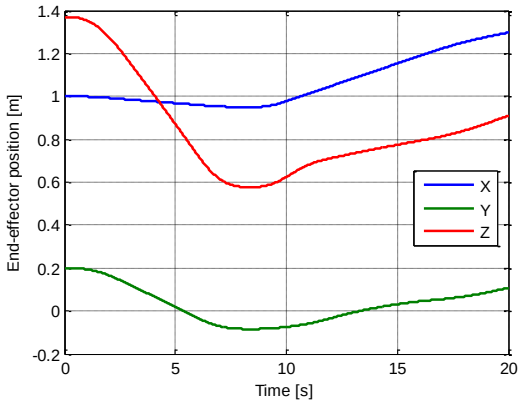

Figure 10 End-effector trajectory in the inertial reference frame

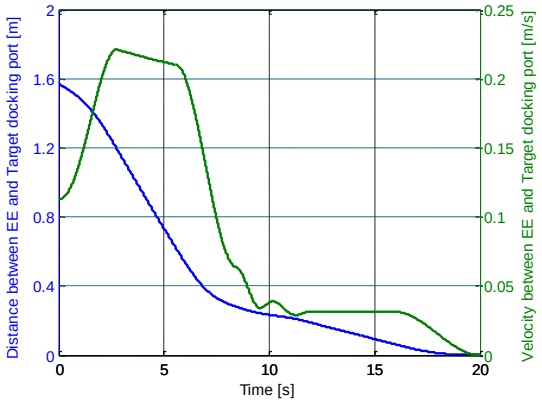

Figure 11 Relative distance and relative velocity between the end-effector and target satellite docking port

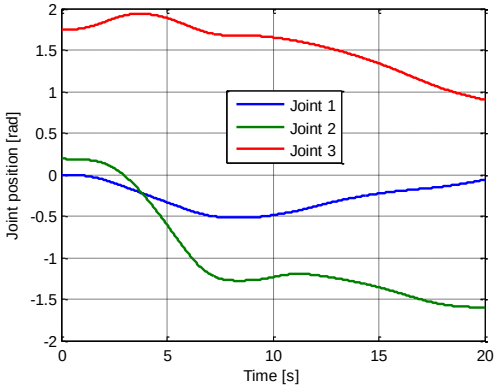

Figure 12 Positions of first three manipulator joints

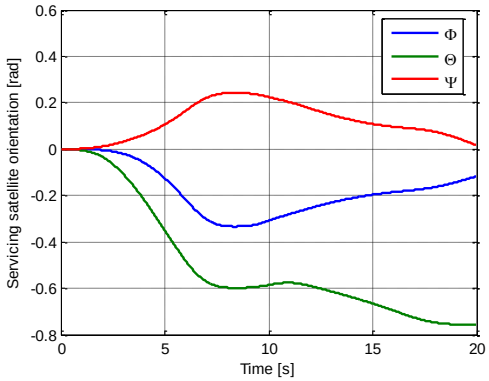

Figure 13 Servicing satellite orientation

4.3 CASE C - Spacecraft-asteroid rendezvous manoeuvre

Another simulation was performed to analyze rendezvous of the manipulator-equipped spacecraft with an asteroid. The same parameters of the system were assumed as in the case of servicing manoeuvre. In this case, however, longer but lighter manipulator was taken into account (3.02 m, 15.1 kg). Performed simulation begins with the end-effector positioned on the asteroid surface (point B on Fig. 2) and finish when the spacecraft has zero relative linear velocity. This is a half of stage 2 in scenario defined in section 2.2. The another

half is more less symmetrical and the motion from point A to point B as well as from point B to point C is the same as in stage 1 in CASE B simulation.

In the preliminary analyzes described in this paper it was assumed that the end-effector cannot move in respect to the asteroid surface and no contact issues were investigated. Manipulator is used to slow-down the spacecraft (from its initial velocity of about 15 cm/s) and to stop its motion in respect to the asteroid surface. Spacecraft position during the maneuver (in respect to its initial position) is presented in the Fig. 14, while spacecraft velocity is shown in the Fig. 15. As can be seen from these figures, spacecraft is slowed to zero on the distance of about 1.5 m. Positions of manipulator joints are presented in the Fig. 16, while their velocities are presented in the Fig. 17. Only joint 2, 3 and 4 are performing motion (position of three remaining joints are zero). Driving torques applied on manipulator joints are shown in the Fig. 18. Maximal torque applied during the maneuver is ~11 Nm.

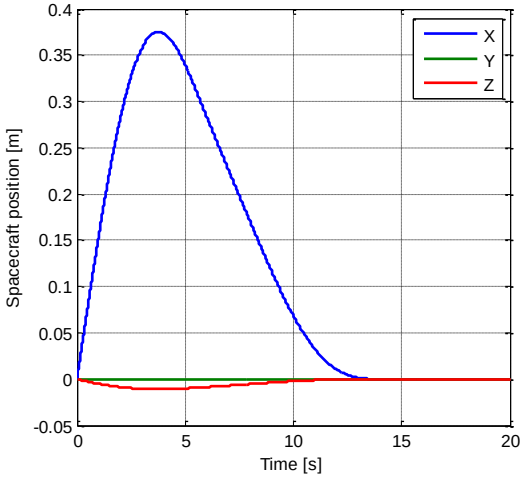

Figure 14 Spacecraft position

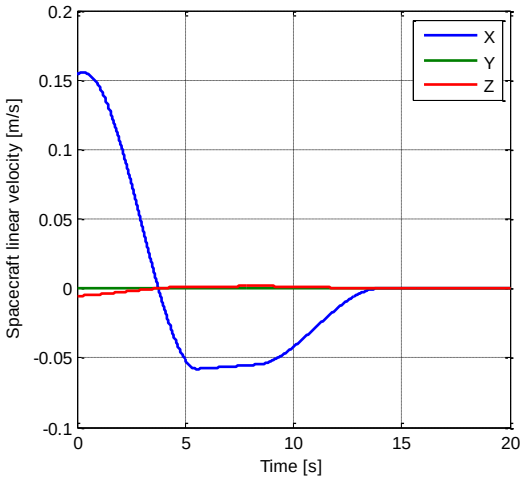

Figure 15 Spacecraft linear velocity

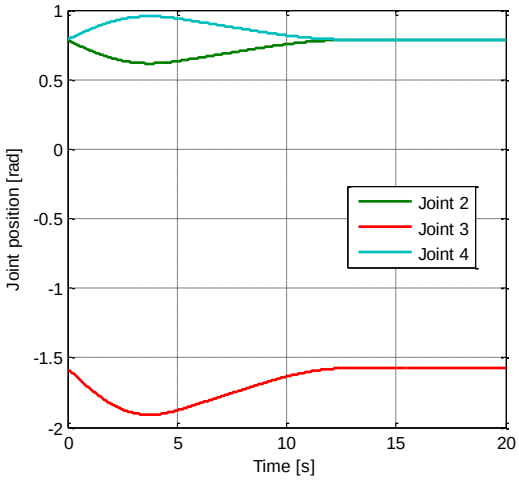

Figure 16 Positions of manipulator joints

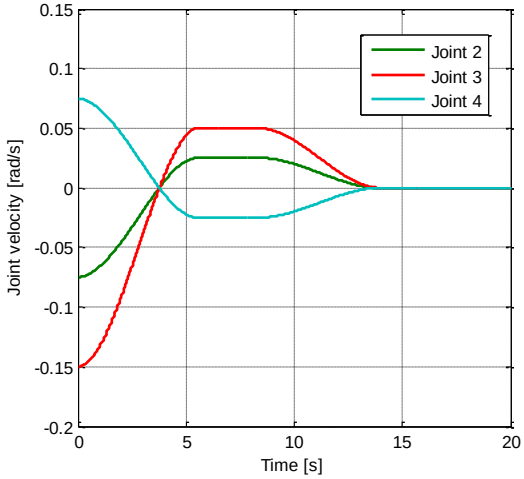

Figure 17 Velocities of manipulator joints

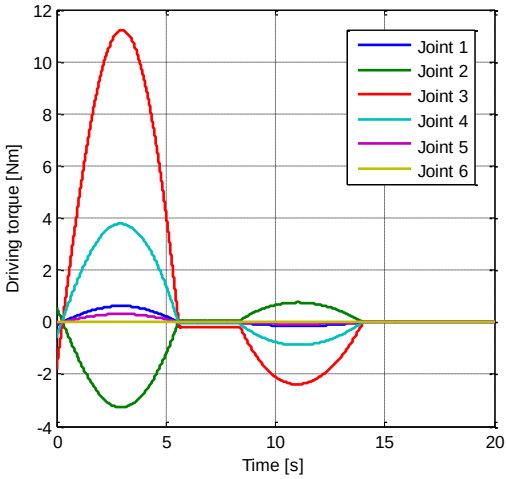

Figure 18 Driving torques applied in manipulator joints

5. CONCLUSIONS AND FUTURE WORK

In the paper the two different applications of the space robots path planning and control theory are described.

First application is related to the servicing maneuvers, where chaser spacecraft should connect to the target satellite using manipulator arm. The second application is connected with spacecraft – asteroid close proximity maneuvers (sometimes called "touch and go" maneuvers) where manipulator positioned some devices on the asteroid surface when spacecraft is in its close proximity. The analysis were based on simulations as well as, in one case on testing using air bearing test-bed system.

The summary of the results and correlated future plans are as follows:

- The results from the test on air bearing test-bed system are qualitatively representative. The identification parameters (e.g. friction in the joints) are needed to quantify the results
- The simulations and test results indicate that, during short time frame (up to 40s) the measurements of the inertial position of the target point are not necessary. Such an approach could be considered as a backup solution for measurement system.
- The 3m length manipulator with appropriate control system is strong enough to extend the sampling process up to 20-30 s. During exemplary simulation the torque in the joints not exceed 11 Nm.

6. ACKNOWLEDGMENTS

This paper was partially supported by the polish National Centre for Research and Development project no. LIDER/10/89/L-2/10/NCBIR/2011.

7. REFERENCES

1. Ellery, A., Kreisel, J. and Sommer, B. (2008). The case for robotic on-orbit servicing of spacecraft: spacecraft reliability is a myth. *Acta Astronautica* 63: 632-648.
2. Yasaka, T. and Ashford, W. (1996). GSV: An Approach Toward Space System Servicing. *Earth Space Review* 5 (2), 9 – 17.
3. Wenfu Xu, Bin Liang, Dai Gao, and Yangsheng Xu (2010). A Space Robotic System Used for On-Orbit Servicing in the Geostationary Orbit. In *Proc. 2010 IEEE/RSJ International Conference on Intelligent Robots and Systems*, Taipei, Taiwan.
4. Visentin, G. and Brown, D.L. (1998). Robotics for Geostationary Satellite Servicing. *Robotics and Autonomous Systems* 23, 45 – 51,
5. Rybus, T. and Seweryn, K. (2013). Trajectory planning and simulations of the manipulator mounted on a free-floating satellite. In *Aerospace Robotics, GeoPlanet: Earth and Planetary Sciences*, Ed. Jurek Z. Sasiadek, Springer-Verlag, 2013.
6. Rebele, B., Krenn, R. and Schäfer, B. (2002). Grasping Strategies and Dynamic Aspects inSatellite Capturing by Robotic Manipulator. In *Proc. 7th ESA ASTRA Workshop*, ESTEC, Noordwijk, The Netherlands.
7. Rybus, T., Seweryn, K., Banaszkiewicz, M., Macioszek, K., Maediger, B. and Sommer, J. (2012). Dynamic simulations of free-floating space robots. In *Robot Motion and Control 2011, Lecture Notes in Control and Information Sciences* 422, Ed. Krzysztof. R. Kozłowski, Springer-Verlag, 351 - 361.
8. Rybus, T., Lisowski, J., Seweryn, K. and Barcinski, T. (2012). Numerical Simulations and Analytical Analysis of the Orbital Capture Maneouvre as a Part of the Manipulator-Equipped Servicing Satellite Design. *In Proc. 17th International Conference on Methods and Models in Automation and Control 'MMAR'2012'*, Miedzyzdroje, Poland, 2012.
9. Skocki, K. Seweryn, K. Kucinski, T. Grygorczuk, J. Rickman, H. Morawski, M. (2012) Experimental determination of the Geotechnical Parameters of planetary bodies – CHOMIK sampling device example. *LPSC XLIII*, The Woodlands, USA.
10. Barucci, M. A. and MarcoPolo-R team. (2012) Proposal of the Near Earth Asteroid Sample Return Mission – MarcoPolo-R. *ESA website*.
11. Seweryn, K., Banaszkiewicz, M., Maediger, B., Rybus, T. and Sommer, J., "Dynamics of Space Robotic Arm During Interactions with Non-Cooperative Objects." In *Proc. of the ASTRA Workshop*, ESTEC, Noordwijk, The Netherlands, 2011.
12. Seweryn, K. and Banaszkiewicz, M. (2008). Optimization of the trajectory of an general free – flying manipulator during the rendezvous maneuver. In *Proc. AIAA Guidance, Navigation and Control Conference and Exhibit 2008*, Honolulu, Hawaii, USA.
13. Menon, C., Busolo, S., Cocuzza, A., Aboudan, A., Bulgarelli, A., Bettanini, C., Marchesi, M. and Angrilli, F. (2007). Issues and solutions for testing free-flying robots. *Acta Astronautica* 60 (12), 957-965.
14. Rybus, T., et al. (2013). New Planar Air-bearing Microgravity Simulator for Verification of Space Robotics Numerical Simulations and Control Algorithms. In *Proc. 12th ESA Symposium on Advanced Space Technologies in Robotics and Automation 'ASTRA 2013'*, ESTEC, Noordwijk, The Netherlands.
15. Dubowsky, S. and Papadopoulos, E. (1993) The Kinematics, Dynamics and Control of Free-flying and Free-floating Space Robotic Systems. *IEEE Transactions on Robotics and Automation* 9 (5), 531 - 543.
15. Umetani, Y. and Yoshida, K. (1989). Resolved Motion Rate Control of Space Manipulators with Generalized Jacobian Matrix. *IEEE Transactions on Robotics and Automation* 5 (3), 303 - 314.